修 士 論 文 の 和 文 要 旨

研究科・専攻	大学院　情報理工学研究科　情報・ネットワーク工学専攻　博士前期課程		
氏　　名	川口　達広	学籍番号	1731053
論 文 題 目	環境発電を用いた通信システムのための 高効率 MAC プロトコルの実環境特性に関する研究		

要 旨

近年，広範囲の環境情報を効率的に長期間観測する技術として，無線センサネットワーク (WSNs: Wireless Sensor Networks) への注目が高まっている．さらに各センサ端末にエナジーハーベスティング (EH: Energy Harvesting) 電源を具備することで，半永久的に情報を取得可能な WSNs の実現が期待されている．しかし，EH 電源のみを用いた WSNs では，各端末は一次電池ではなく，自然界から回収される電力のみによって動作するため，各端末の動作電源は微弱かつ確率的に変動する性質をもつ．そのため各端末の消費電力が EH 電源からの回収電力を上回った場合は，各端末が電池切れを引き起こし，ネットワークが動作不能となることが懸念される．よって，各端末の電池切れに対してロバスト性をもち，通信の必要が生じた時のみ通信を行うことで，省電力性を達成する方式が必要となる．

媒体アクセス制御 (MAC: Medium Access Control) 層における研究では，端末間の時間同期を行うことなく，日和見的に通信を行う受信機駆動型 MAC が検討されている．特に，Intermittent-receiver driven data transmission (IRDT) は，高い省電力性と通信品質を達成する通信方式として知られている．IRDT は，各端末の供給電力が確率的に変動することを考慮していない．そのため，EH 電源を用いた WSNs においては，回収電力が小さい端末が動作不能に陥る可能性があり，通信品質の劣化を引き起こす．そこで IRDT に対して，EH 電源からの回収電力の多寡と通信可能端末数の情報を用いて，適応的に各端末が間欠間隔を制御することで消費電力制御を可能にした Energy-Neutral Receiver-Initiated MAC (ENRI-MAC) が提案されており，IRDT に比べ，高い通信品質を達成可能であることが示されている．しかし，ENRI-MAC の特性評価は，各端末の回収電力を 3 つのクラスタに分類することで回収電力の多寡を考慮した擬似的なモデルで性能評価を行ったものであり，実環境に則して空間的・時間的に回収電力が変化するモデルにおいて，同様に高い通信品質を達成するかについては議論の余地がある．

そこで本研究では，ENRI-MAC の間欠間隔の動的制御機能が通信品質を改善し得るかを評価するため，実環境の回収電力モデルに即した特性評価を行う．回収電力は環境的要因により変動し，同一の実験環境で評価することが困難であるため，今回は実環境に多数の照度センサを配置することで，日中の照度を実測し，この値を回収電力の実測値として用いた計算機シミュレーションを行う．数値評価を通じて，実環境では，間欠間隔の伸延を行うことで自端末の消費電力を低減する機能が，他端末の消費電力を著しく増加させてしまい，ネットワーク内に電池切れを連鎖的に引き起こし，通信品質を劣化させる可能性があることを明らかにする．

この問題を解決するために，本稿では ENRI-MAC において提案される間欠間隔設計を見直すことで，回収電力を ENRI-MAC よりも効率的に利用可能な間欠間隔を制御可能改良された改良 ENRI-MAC を提案する．さらに，先に述べた実環境に即した回収電力モデルにおいて，提案する改良 ENRI-MAC の間欠間隔設計が高い通信品質を達成可能であることを示す．

平成30年度　修士論文

Experimental Evaluation of Highly-Efficient Medium Access Control Protocol for Energy Harvesting Communications Systems

環境発電を用いた通信システムのための高効率MACプロトコルの実環境特性に関する研究

学籍番号　1731053

氏　名　川口　達広

指導教員　石橋　功至 准教授

電気通信大学　情報理工学研究科

情報・ネットワーク工学専攻

提出日　平成31年3月14日

Abstract

This paper focuses on asynchronous receiver-initiated medium access control (MAC) protocol for energy-harvesting wireless sensor networks. A protocol named *energy-neutral receiver-initiated MAC* (ENRI-MAC) enables every sensors to autonomously decide its own intermittent interval based on both available energy from the energy harvester and the number of sensors in the coverage. However, the original ENRI-MAC may cause a catastrophic situation that nodes in the coverage would run out of their batteries due to the chain reaction of energy scarcity through autonomous control of intermittent interval. To this end, we propose improved ENRI-MAC that can control the intermittent interval so as to exploit available energy more than original ENRI-MAC. In order to evaluate the performance of improved ENRI-MAC, we experimentally measure illuminances in a large-scale environment, and perform computer simulations based on this measurement model with photovoltaic model.

Contents

Abstract **i**

1 Introduction **2**
1.1 Background . . . 2
1.2 Organization . . . 3

2 System Model **4**
2.1 Device Model . . . 4
2.2 Wireless Channel Model . . . 5
2.3 Network Model . . . 7

3 Receiver-Initiated MAC Protocol **8**
3.1 IRDT . . . 8
3.1.1 Rx: DATA receiving mode . . . 9
3.1.2 Tx: DATA transmitting mode . . . 10
3.2 Theoretical Analysis . . . 12
3.2.1 Performance of wireless communications . . . 12
3.2.2 Energy consumption of network . . . 14

4 Improved Energy-Neutral Receiver-Initiated MAC Protocol **17**
4.1 Energy-aware load control . . . 18
4.2 Observation of peripheral condition . . . 20

5 Evaluation of Protocols with Empirical Model of Distributed Photovoltaics **22**
5.1 Experimental setup for evaluating . . . 22
5.2 Empirical Model of Energy Harvesting . . . 24
5.2.1 Experimental device . . . 24
5.2.2 Photovoltaics output model . . . 24
5.3 Numerical results . . . 27

6 Conclusions **29**

Appendix **30**

Acknowledgments **34**

List of Publications **35**

Chapter 1

Introduction

1.1 Background

Wireless sensor networks (WSNs) have gained much attention for collecting a vast amount of environmental information for a long period [1]. The technology has been mainly used in monitoring platform for infrastructure. Figure.1.1 illustrates an overview of WSNs. In WSNs, it is possible to gather environmental information by utilizing a massive number of wireless sensor nodes (SNs) equipping wireless devices. SNs are often battery-powered, and hence extending the network lifetime is one of the primary concerns in the deployment of WSNs. Especially, when SNs collect a wide range of information, it is necessary to extend the communication distance, and the increasing in power consumption for transmission becomes a critical problem; thus, each wireless sensor node (SN) gets sensing information (DATA) and sends to Gateway (GW) using multi-hop communication [2]. However, even if the power consumption of communications is reduced, each SN still has the limitation of the pre-charged battery. Once the charged amount of the battery runs out, the battery replacements are required. This enormous maintenance cost of the replacements becomes a big issue for realizing WSNs. In order to overcome the limitation, energy-harvesting WSNs (EHWSNs) have been proposed [3], where SNs can operate with only energy-harvesting (EH) power sources. EH power sources harvests energy from ambient sources, *e.g.*, sunlight, wind, microwave. It is expected that *chargeless networks* can be realized by using EH power resources. However, EH are a stochastic power resource; hence, SNs have to wait for a certain period of time to store up enough energy in order to communicate with each other.

One of the solutions is a duty cycle control system in medium access control (MAC) layer [4].

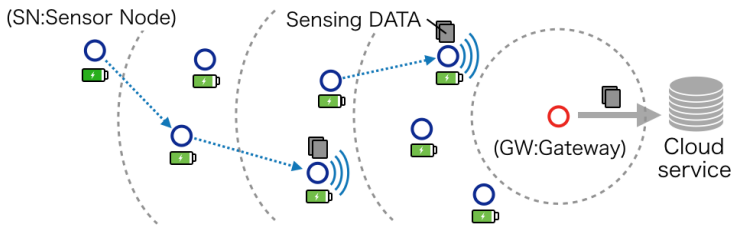

Figure 1.1: Wireless sensor networks

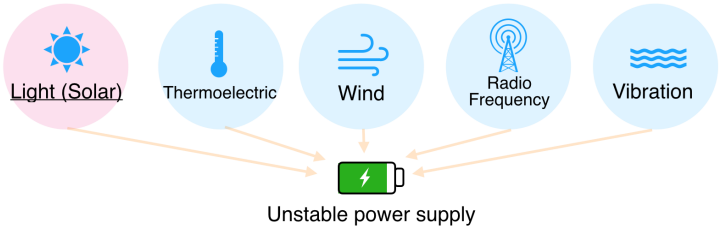

Figure 1.2: Energy-harvesting

In the literature [5], asynchronous duty cycle control protocol, called Receiver-Initiated MAC (RI-MAC) has been proposed. In this system, when not communicating with, the SN maintains a sleep mode to save energy and activates only when communications are required. After that, the literature [6] has proposed intermittent receiver-driven data transmission (IRDT) protocol to improve the energy-efficiency performance of RI-MAC, in which IRDT protocol uses short link-message before sending DATA. IRDT protocol is more energy-efficient receiver-initiated MAC protocol compared to RI-MAC. However, while it can also achieve high packet delivery ratio (PDR), IRDT protocol does not consider the remaining energy in super-capacitor or the available energy from energy harvester, so that it is not appropriate to use the method as it is for EHWSNs.

In conventional research, an improved protocol of IRDT, *energy-neutral receiver-initiated MAC* (ENRI-MAC) has been proposed for EHWSNs [7]. ENRI-MAC enables every sensors to autonomously decide its own intermittent interval based on both available energy from the energy harvester and the number of sensors in the coverage. While ENRI-MAC achieves high PDR in theoretical analysis, the performance of real environment is not guaranteed since an energy-harvesting power supply is a complex and stochastic power source. Therefore, we evaluate the performance of ENRI-MAC using the energy-harvesting model based on actual measurement data. However, the original ENRI-MAC may cause a catastrophic situation that nodes in the coverage would run out of their batteries due to the chain reaction of energy scarcity through autonomous control of intermittent interval. To this end, we propose improved ENRI-MAC that can control the intermittent interval so as to exploit available energy more than original ENRI-MAC. In order to evaluate the performance of improved ENRI-MAC, we experimentally measure illuminances in a large-scale environment, and perform computer simulations based on this measurement model with photovoltaic model.

1.2 Organization

The remainder of this thesis is organized as follows. System model for evaluation is defined in chapter 2. Chapter 3 and 4 is dedicated to introducing IRDT and the improved ENRI-MAC. Chapter 5 shows the performance of improved ENRI-MAC based on an empirical model of distributed photovoltaics. We show the effectiveness of energy-neutral control system by comparing IRDT with improved ENRI-MAC. Finally, chapter 6 concludes our research.

Chapter 2

System Model

2.1 Device Model

WSNs consisted of SNs with EH system. The device model is shown in Fig.2.1. EH system harvests energy $q_s(t)$ [W] from photovoltaics. Let, t stands for time. The parameter $q_s(t)$ is based on actual measured data. In actual devices, we cannot ignore energy loss due to a power conversion like DC/DC convertor, so that η $(0 < \eta < 1)$ is defined as a conversion efficiency factor. We assume that each SN can know the information on instantaneous harvested power $\eta q_s(t)$ and the remaining battery capacity $Q_{st}(t)$ [J]. Each SN generates a data packet (DATA) from a sensor with certain interval denoted as T_g. In addition, each SN operates based on MAC protocol detailed in the next section.

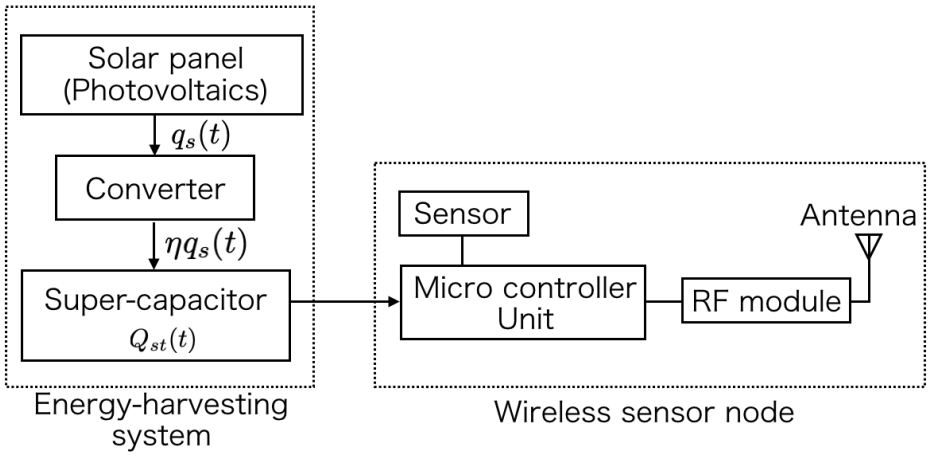

Figure 2.1: Device model

Table 2.1: Wireless channel parameter

Frquency band [MHz]	920
Transmitted power P_t [dBm]	0
Antenna gain G_r, G_t [dBi]	-1.6
Antenna receive sensitivity P_{th} [dBm]	-100
Receiver antenna height h_r [m]	0.237
Transmitter antenna height h_t [m]	0.237

2.2 Wireless Channel Model

In Japan, the 920 MHz band is an unlicensed band and is expected to be effectively used in WSNs in the future. Hence, we consider the parameters of *IEEE802.15.4g Standard Low Power Sub-GHz Radio Module - BP3596A* [8]. The parameters is shown in Table.2.1. Besides, it is assumed that when we construct WSNs, we put the sensors near the ground, so that we have to consider the attenuation caused by decreasing the Fresnel radius. Therefore all wireless channel link is based on empirical model. Figure 2.2 shows receiver signal strength indication (RSSI) in the actual environment. The actual RSSI is measured in Line-of-sight propagation using BP3596A.

The theoretical curve of the two-rays ground reflected model is also described in the result. The received power of the model in decibels can be written by

$$P_r = \left\{ \frac{\lambda}{2\pi d} \sin\left(\frac{\Delta\phi}{2}\right) \right\}^2 G_r G_t P_t. \tag{2.1}$$

Let, $\Delta\phi \approx (4\pi h_r h_t)/\lambda d$. P_t is transmitted power. λ is wavelength, and d[m] denotes distance between nodes. h_r denotes receiver antenna height. h_t is transmitter antenna height. All SNs and GW equip a single isotropic antenna. The receiver antenna gain is G_r. The transmitter antenna gain is G_t. For simplicity, it is assumed that packets are correctly received as long as the received signal power P_r exceeds a given receiver sensitivity P_{th}. We further assume that packets exceeding P_{th} may collide with each other and the collided signals cannot be demodulated correctly, while those below P_{th} do not interfere. Moreover, we assume that carrier sense is always performed before transmission; if the received power exceeds P_{th}, the transmitter can perfectly recognize the existence of other transmitters, and waits for transmission until other transmitters finish transmissions.

Comparing with measured values in line of sight environment, the results shows that each node can communicate within 50[m].

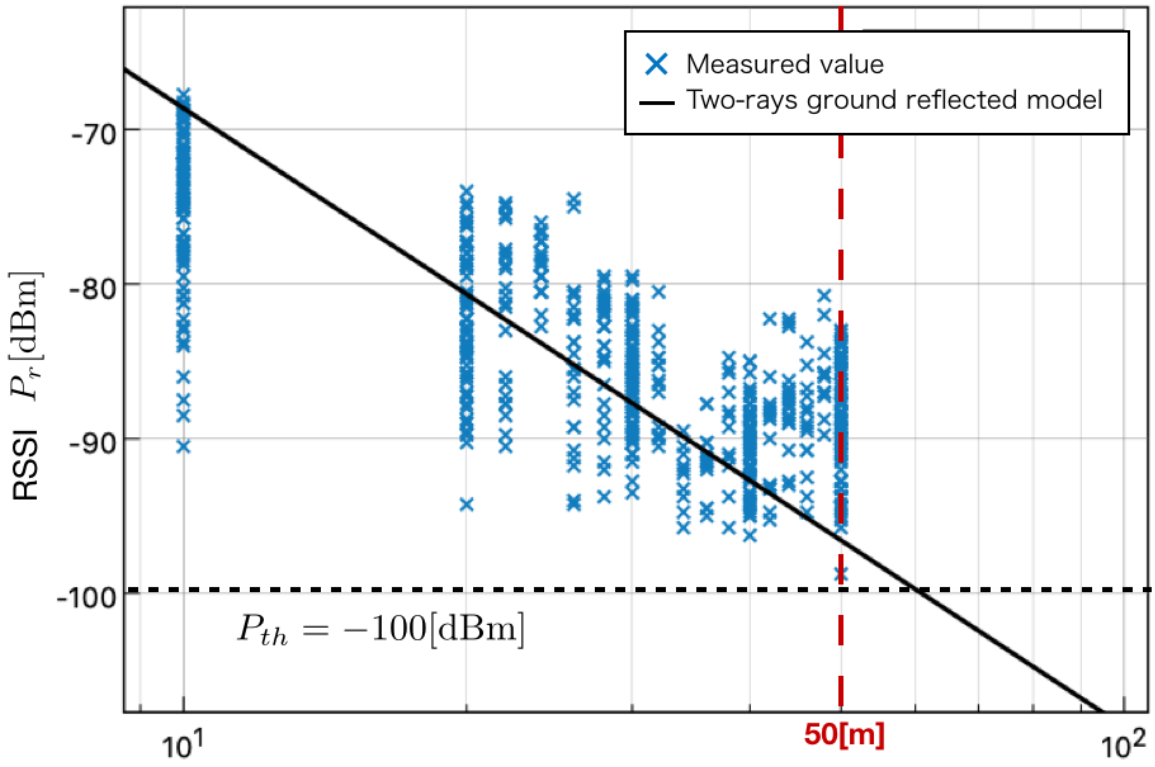

Figure 2.2: Receiver signal strength indication in the actual environment; a black dot line in the figure denotes antenna receive sensitivity. A red line shows communication distance.

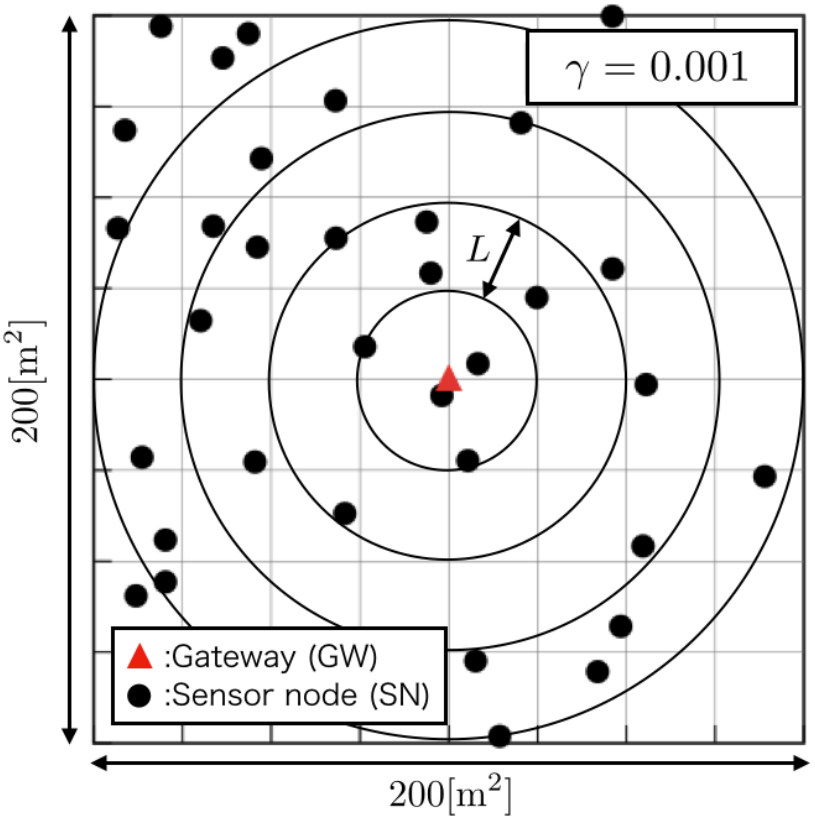

Figure 2.3: Network model

2.3 Network Model

We consider $Z = 200$ [m] $\times$ 200 [m], two-dimensional Euclidean space. The network consists of a common gateway (GW) and SNs, and positions of SNs are modeled by poison point process (PPP) [9] which is commonly used in WSNs. N denotes the number of SNs. N follows a probability of

$$U(X = x) = \frac{\gamma^x e^{-\gamma}}{x!}. \tag{2.2}$$

e represents the number of Napier and γ is a density of PPP. Note that, the average number of SNs in the network is given by $\overline{N} = \gamma Z$. Each SN-i is categorized into $\alpha^{(i)}$ clusters, where i is an index of node-number. In a word, a cluster-number of node-i denotes $\alpha^{(i)}$. Each cluster-number is decided by the distance from the GW when the SN is installed in environment. GW belongs to 0-th cluster, $\alpha^{(\mathrm{D})} = 0$. D is an index of GW. Let, r is the distance between SN-i and GW, $\alpha^{(i)}$ satisfies $(\alpha^{(i)} - 1)L < r \leq \alpha^{(i)}L$. L denotes cluster range. Figure 2.3 shows one example of PPP distribution model.

Chapter 3

Receiver-Initiated MAC Protocol

This chapter describes IRDT [10] which is the basis of the improved ENRI-MAC. Firstly, we introduce the algorithm of IRDT, then we explain its performance with theoretical analysis.

3.1 IRDT

IRDT is a kind of the asynchronous RI-MAC and achieves higher energy-efficiency performance than original RI-MAC [5]. In IRDT, the SN maintains a sleep mode to save energy and starts up only when communication is required. As shown in 3.1, the operations in IRDT protocol can be divided into two modes, namely a DATA transmitting mode (**Tx**), and a DATA receiving mode (**Rx**). Every SN is usually sleeping and awakes every intermittent-interval $T_R^{(i)}$ and decides to be **Tx** or **Rx**. Let $T_R^{(i)}$ denote the intermittent interval of the i-th node. The SN operates as **Tx** if the node possesses DATA; otherwise, the SN operates as **Rx**.

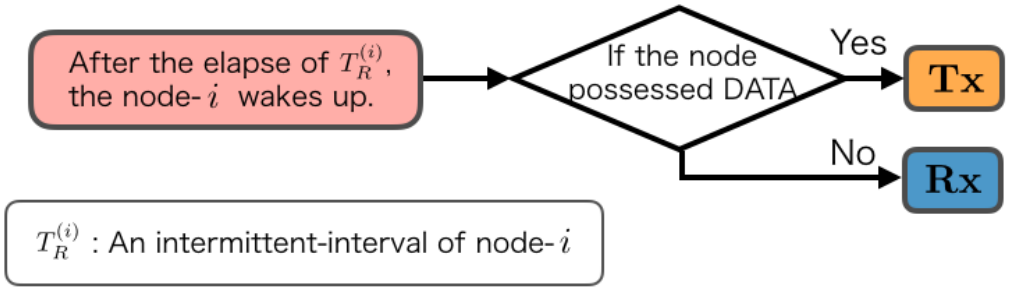

Figure 3.1: Operation at startup of IRDT protocol

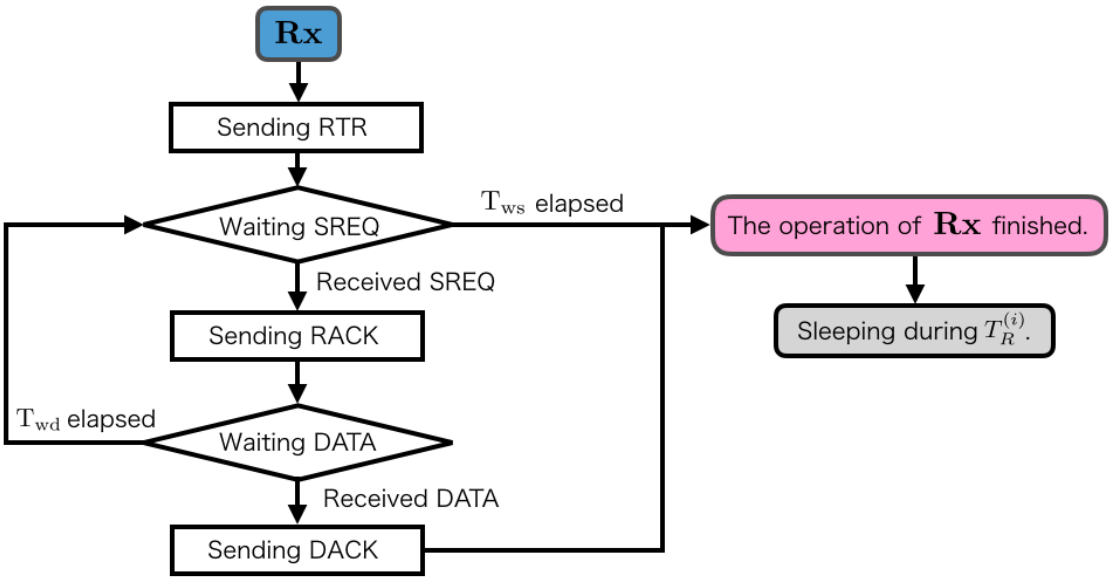

Figure 3.2: Operation as **Rx**

3.1.1 Rx: DATA receiving mode

Figure 3.2 shows the procedure of **Rx**. When the SN becomes **Rx**, it broadcasts Ready To Receive (RTR) signals to inform neighboring SNs that the SN is ready for receiving DATA. If the SN has sent RTR which includes their belonging area-number, it starts waiting Send Request for DATA (SREQ) signal from **Tx**. If the SN receives SREQ, it sends ACKnowledgement for SREQ (RACK) signal and makes a link. After making the link, the SN waits DATA. If it gets DATA, it transmits Data ACKnowledge (DACK) signal to **Tx**. If the SN gets DATA, it starts up as **Tx** next. GW does not operate as **Tx**, and just performs as **Rx**.

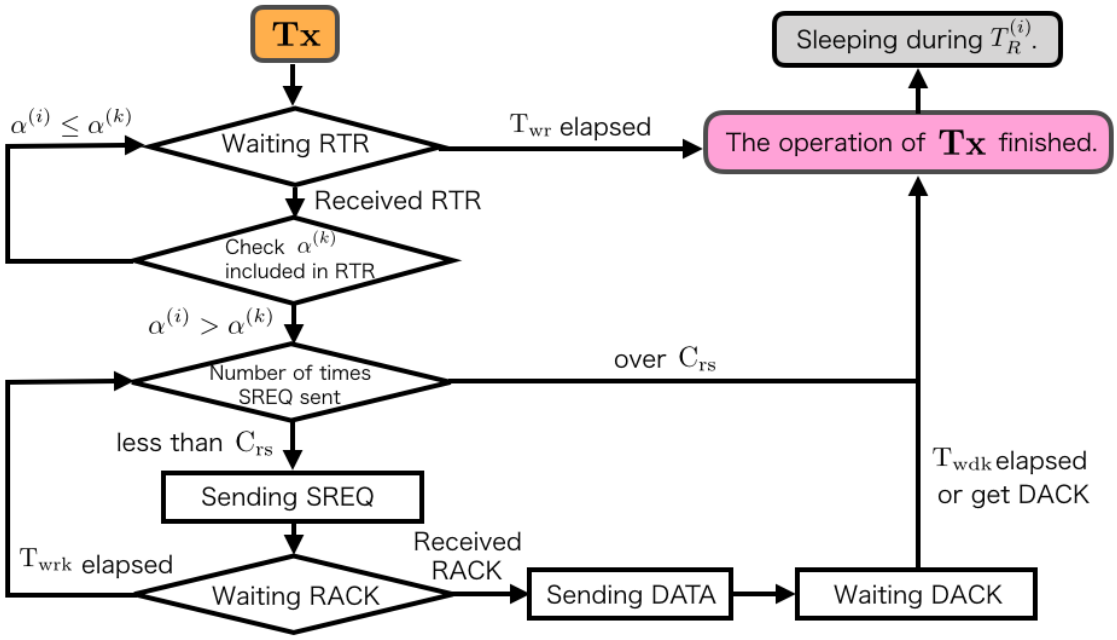

Figure 3.3: Operation as**Tx**

3.1.2 Tx: DATA transmitting mode

If the SN-i in **Tx** mode and belongs to area alpha (i) receives from lower area $\alpha^{(k)}$, the SN-i transmits SREQ against SN-k. Each SN sends DATA to other SNs belonging to areas which is closer to GW using the area-number α. C_{rs} denotes the retransmission counter of SREQ. After receiving the RACK that is received from SN-k, it transmits DATA. Finally, when receiving DACK from **Rx**, communication is terminated. Besides, if the time T_{wr} has elapsed, the DATA is discarded. Figure 3.4 illustrates the basic procedure of IRDT protocol in the time axis.

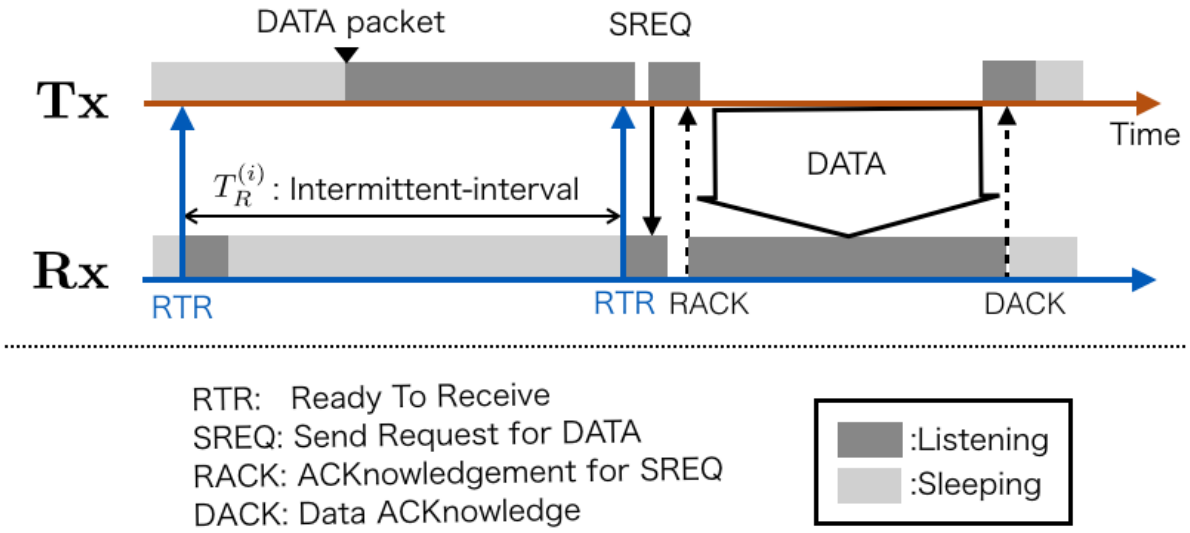

Figure 3.4: Basic procedure of IRDT protocol; every arrow in the figure denotes a transmission between a node pair.

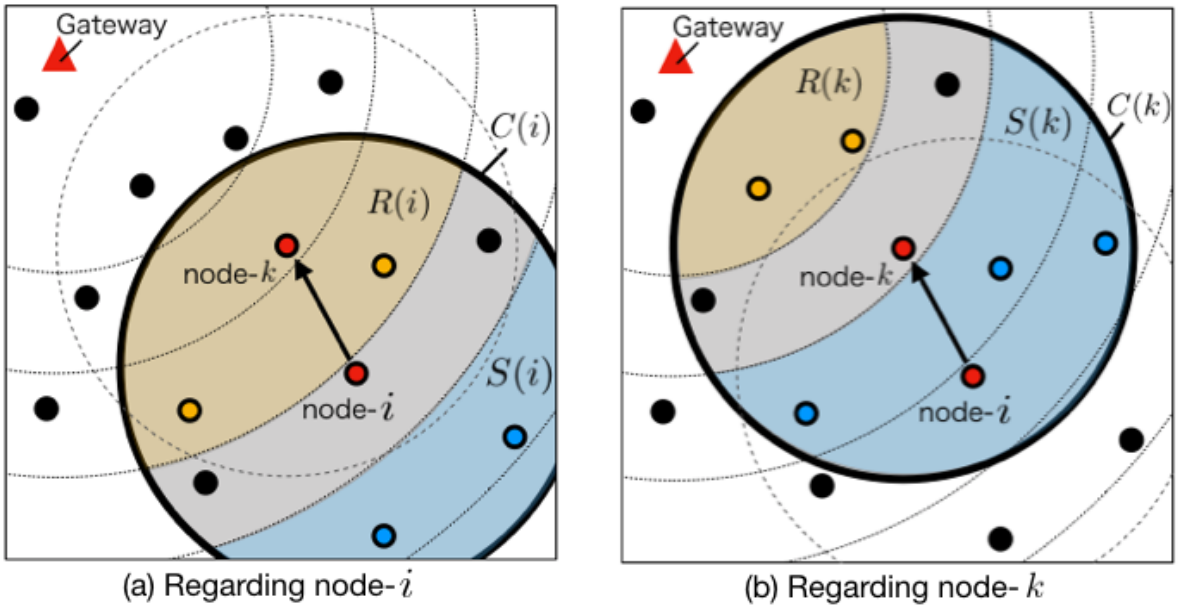

Figure 3.5: One example of a network

3.2 Theoretical Analysis

In this section, we describe the theoretical analysis of the performance of IRDT. For the sake of simplicity, it is assumed that each node operates with no limited battery and packet retransmission is not performed. A theoretical analysis of the performance of IRDT is shown in the paper [11]. We modify these approximate analytical expressions to faithfully appropriate form to assumed models. These equations show End To End packet loss rate (PLR) and energy consumption of the whole network. This analysis guarantees not only the performance of IRDT but also the improved ENRI-MAC. Figure 3.5 illustrates a part of assumed networks. i, j, k, l, m, and n denote index of SN. $C(i)$ denotes set of SNs which the i-th SN can communicate with. Within $C(i)$, SNs which are belonging to the upper cluster is denoted by set $S(i)$, and SNs which are belonging to the lower level cluster is denoted by set $R(i)$.

3.2.1 Performance of wireless communications

Firstly, we shows the packet loss probability of communications. Since it is assumed that each short packet is ideally error-correctable, we do not consider the collisions between RTR, SREQ, RACK and DACK signals. Note that Signal collision occurs between the hidden SNs, where communication fails if RTRs from other hidden terminals collide while transmitting DATA. We call this scenario *RTR-collision* scenario. $P_R^{i\to k}$ is packet loss probability (PLP) from node-i to node-k caused by *RTR-collision* scenario. $P_R^{i\to k}$ is given by

$$P_R^{i\to k} \approx 1 - \prod_{j\in C(k)\setminus C(i),\{i\}} \left(1 - \frac{\mathrm{T_d}}{T_R^{(j)}}\right), \tag{3.1}$$

where $\mathrm{T_d}$ is required time for DATA transmission In addition to *RTR-collision* scenario, communication also fails when *SREQ-collision* scenario occurs. When an available RTR is received at the same time in multiple **Tx**, a communication fails by a collision of SREQs. ρ_i is packet possession probability of node-i. Let, ρ_i of edge node is $1/\mathrm{T_g}$. Let us denote $P_e^{i\to k}$ denoted as the PLR from node-i to node-k. ρ_i is given by

$$\rho_i \approx \frac{1}{\mathrm{T_g}} + \sum_{n\in S(i)} \frac{\beta_l}{T_R^{(i)}} \rho_l (1 - P_e^{l\to i}). \tag{3.2}$$

Parameter $\beta^{(l)}$ represents a probability that each terminal is selected as a communication partner. $\beta^{(l)}$ has a constraint condition of $\sum_{m\in R(l)} \frac{\beta_l}{T_R^{(m)}} = 1$.

$P_S^{i\to k}$ is PLP caused by *SREQ-collision* which is given by

$$P_S^{i\to k} \approx \sum_{t=1}^{T_R^{(i)}} \frac{1}{T_R^{(i)}} \left\{ 1 - \prod_{n\in S(k)\setminus\{i\}} (1-\rho_l)^t \right\}. \tag{3.3}$$

Since the load of communication concentrates only at GW, the above approximation formula can not be applied. Therefore, following expressions

$$p_{T_R(\mathrm{D})}^{i\to \mathrm{D}} = 1 - \prod_{n\in S(\mathrm{D})\setminus\{i\}} (1-\rho_k)^t, \tag{3.4}$$

$$P_S^{i\to \mathrm{D}} = \sum_{t=1}^{T_R^{(\mathrm{D})}} \frac{1}{T_R^{(D)}} \left[p_{T_R^{(\mathrm{D})}-t}^{i\to \mathrm{D}} + \{1 - p_{T_R^{(\mathrm{D})}-t}^{i\to \mathrm{D}}\} p_{T_R^{(\mathrm{D})}-t}^{i\to \mathrm{D}} \right] = p_{T_R^{(\mathrm{D})}}^{i\to \mathrm{D}}, \tag{3.5}$$

are used, where GW node is denoted as D. Following the above mentioned equations, $P_S^{i\to k}$ is redefied as

$$P_S^{i\to k} \approx \begin{cases} p_{T_R^{(\mathrm{D})}}^{i\to \mathrm{D}} & (k = \mathrm{D}) \\ \sum_{t=1}^{T_R^{(i)}} \frac{1}{T_R^{(i)}} \left\{ 1 - \prod_{n\in S(k)\setminus\{i\}} (1-\rho_l)^t \right\} & (\text{otherwise}). \end{cases} \tag{3.6}$$

If $P_e^{i\to k}$ is further defined as a probability which consists both *RTR-* and *SREQ-collision* scenarios, it will be denoted as

$$P_e^{i\to k} = P_S^{i\to k} + (1 - P_R^{i\to k}) P_R^{i\to k}. \tag{3.7}$$

When isolated SNs in the network is considered, in order from the SN-i of the cluster closer to GW, $P_e^{i\to \mathrm{D}}$ is calculated by

$$P_e^{i\to \mathrm{D}} = \begin{cases} 1 & (\text{isolated}) \\ \sum_{l\in R(i)} \frac{\beta_l}{T_R^{(l)}} \left[P_e^{l\to \mathrm{D}} + (1 - P_e^{l\to \mathrm{D}}) \right] & (\text{otherwise}). \end{cases} \tag{3.8}$$

Therefore, PLR of whole network can be written as

$$\overline{P_e} = \frac{1}{N} \sum_{i\in N} P_e^{i\to \mathrm{D}}. \tag{3.9}$$

3.2.2 Energy consumption of network

$E(i)$ is energy consumption SN-i per unit time. Note that, below approximate expressions about $E(i)$ is not satisfied when there are isolated SNs in the network.

$$E(i) = \frac{\mathrm{E_{RTR}}}{T_R^{(i)}} + \left(\rho_i - \frac{1}{\mathrm{T_g}}\right)\mathrm{E_{Rx}} + \rho_i E_{\mathrm{Tx}}, \tag{3.10}$$

where $\mathrm{E_{Rx}}$ is the energy consumption when SN is in mode **Rx**. E_{Tx} is energy consumption in driving as **Tx**. $\mathrm{E_{RTR}}$ represents the energy consumption of a single batch receiving short-time reception after transmitting RTR.

$$E_{\mathrm{Tx}} = \tau \mathrm{E_{recieve}} + \mathrm{E_{DATA}}, \tag{3.11}$$

Let, E_{receive} indicates the energy consumption during the operation of the receiver. E_{DATA} denotes the amount of energy required to transmit DATA. τ is given by

$$\tau \approx \sum_{t=0}^{T_{R,\min}-1} \left[t \left\{ 1 - \prod_{l \in R(i)} \left(1 - \frac{1}{T_R(l) - 1} \right) \right\} \prod_{l \in R(i)} \left(1 - \frac{t}{T_R^{(l)}} \right) \right]. \tag{3.12}$$

Let, $T_{R,\min} = \min_l T_R^{(l)}$. Therefore the average of energy consumption of the whole network is given by

$$\overline{E} = \frac{1}{N} \sum_{i \in N} E(i). \tag{3.13}$$

When the density of SNs in the network is sufficiently large, the theoretical analysis is available. We show the performance of PLR using Monte Carlo simulation. The simulation parameters is shown in Table 3.1. The network model corresponds to Chapter 2.3. As shown in Fig.3.6, IRDT can reduce PLR by designing the intermittent-interval appropriately. When we use IRDT, we need to design properly a density of network for preventing communication quality from declining. In other words, there is an optimum intermittent-interval $\mathrm{T_{R-opt}}$ that minimizes PLR, corresponding to network density. In this system model, we set $\mathrm{T_{R-opt}} = 500$[msec].

Table 3.1: Simulation parameter for theoretical analysis

Transmission rate [kbps]	250
Size of DATA [byte]	26
DATA generation interval T_g[min]	10
Size of RTR and SREQ [byte]	9
Size of RACK and DACK [byte]	8
Maximum listening time T_{ws}, T_{wrk} and T_{wdk} [msec]	5
Maximum listening time T_{wd} [msec]	30
Maximum listening time T_{wr} [min]	10
Counter of SREQ to discard DATA C_{rs}	1
Average current during transmitting [mA]	18.0
Average current during receiving [mA]	13.0

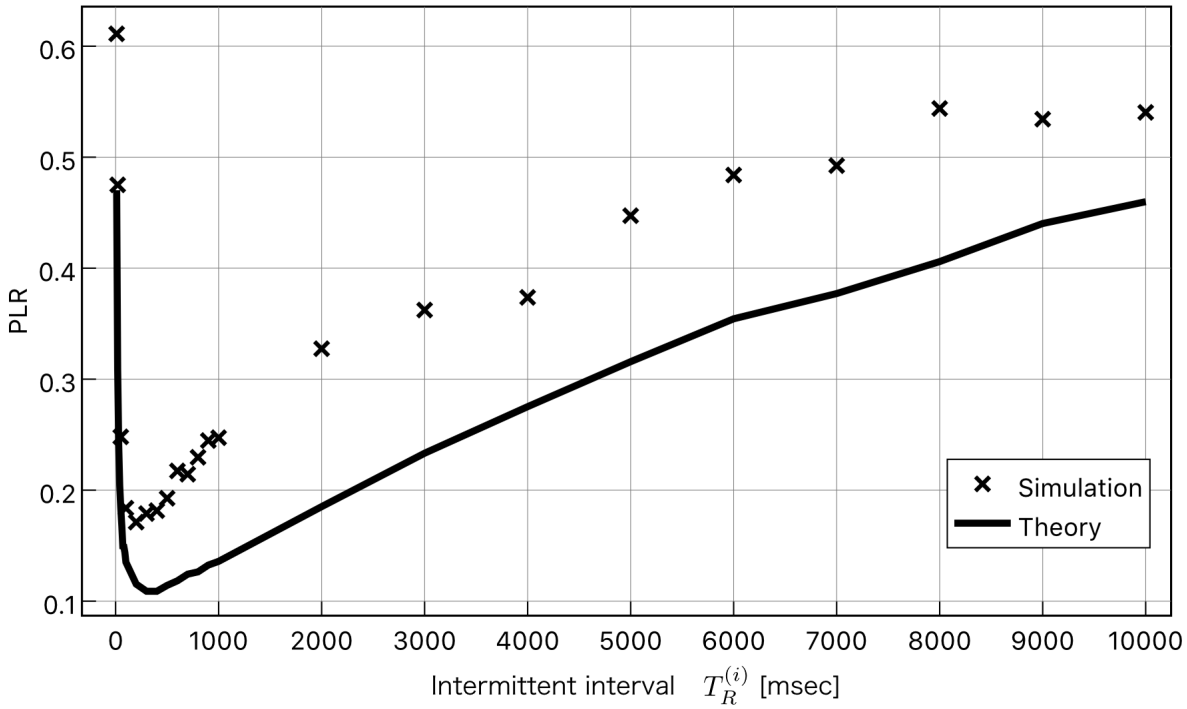

Figure 3.6: PLR of whole network. ($Z = 200[\mathrm{m}] \times 200[\mathrm{m}], \gamma = 0.001, L = 10[\mathrm{m}]$)

Chapter 4

Improved Energy-Neutral Receiver-Initiated MAC Protocol

In this chapter, we introduce improved ENRI-MAC protocol. Firstly, we explain ENRI-MAC [7] briefly. Although ENRI-MAC are an improved protocols of IRDT for EHWSN and shares the basic procedure, operations before and after sleeping differs. ENRI-MAC is a protocol that can achieve energy-neutrality by adopting the following two functions below:

- Energy-aware load control
- Observation of peripheral condition

These functions can autonomously operate at each SN, and above two functions exhibit their performance by controlling its own intermittent interval. If SNs with excess energy should shorten the intermittent interval to T_S, other SNs which operate with the long intermittent interval of T_L can reduce their energy consumption. Let, the threshold for determining the presence or absence of energy denotes $\mathrm{Q_{mid}}$. The system prevents deterioration of communication quality caused by battery exhaustion. One way to determine the intermittent interval is shown in literature [11]. Each SN decides the intermittent interval using the following equations and the theoretical analysis formula shown in section 3.2.

$$T_S = \arg\min \overline{P_e} \tag{4.1}$$

$$T_L = \arg\min \overline{E} \tag{4.2}$$

While we can determine T_S using the theoretical analysis, it is difficult to determine T_L. As shown in fig.3.6, it is clear that it needs to be $T_L \geq T_S$. However, depending on the network density and the communicable distance, there is a possibility that it will be $T_L < T_S$, and we cannot decide T_L properly in such a case. The network model of this paper is also the case. In such a case, T_L can only be set to an arbitrary value. To solve this problem, improved ENRI-MAC differs from ENRI-MAC [7] in that procedure of determining intermittent interval. We explain these functions in the next section.

4.1 Energy-aware load control

Figure 4.2 shows the operation of before going to sleep. To avoid the outage of SN-i due to the scarcity of energy, SN-i checks their remaining battery capacity $Q_{st}(t)$ before going to sleep. When the stored energy from the EH power-supply exceeds the threshold value $\mathrm{Q_{th}}$, it can be judged that the SN-i has sufficient energy for one DATA transmission. $\mathrm{Q_{th}}$ is given by

$$\mathrm{Q_{th}} = \mathrm{Q_{mid}} + \mathrm{E_D}, \tag{4.3}$$

where $\mathrm{E_D}$ denotes the amount of energy consumption for one DATA transmission and $\mathrm{Q_{mid}}$ is half of the maximum operable capacity of the capacitor. The SN-i with enough energy operates with intermittent-interval of $\mathrm{T_{R-opt}}$. Then, $\mathrm{E_D}$ is represented by

$$\mathrm{E_D} = \mathrm{E_{receive}}\mathrm{T_{R-opt}} + \mathrm{E_{DATA}}, \tag{4.4}$$

where $\mathrm{T_{R-opt}}$ is an intermittent-interval for minimizing the PLR which is determined when the network is designed. If the SN-i does not have enough energy, its intermittent-interval is extended so that the SN-i can sleep for a longer period and thus can harvest more energy. T_Θ is calculated by

$$T_\Theta = \begin{cases} \mathrm{T_{R-opt}} & (Q_{st}(t) \geq \mathrm{Q_{th}}) \\ \frac{\mathrm{E_D}}{\eta q_s(t)} & (\text{otherwise}). \end{cases} \tag{4.5}$$

Then, each intermittent-interval $T_R^{(i)}$ is set by

$$T_R^{(i)} = \begin{cases} \mathrm{T_{R-opt}} & (T_\Theta \leq \mathrm{T_{R-opt}}) \\ \mathrm{T_{R-MAX}} & (T_\Theta \geq \mathrm{T_{R-MAX}}) \\ T_\Theta & (\text{otherwise}). \end{cases} \tag{4.6}$$

With this function, it is possible to control the communication load on SNs depending on available energy. Thus control enables to prevent the outage of the network and thus results in the improvement of PLR.

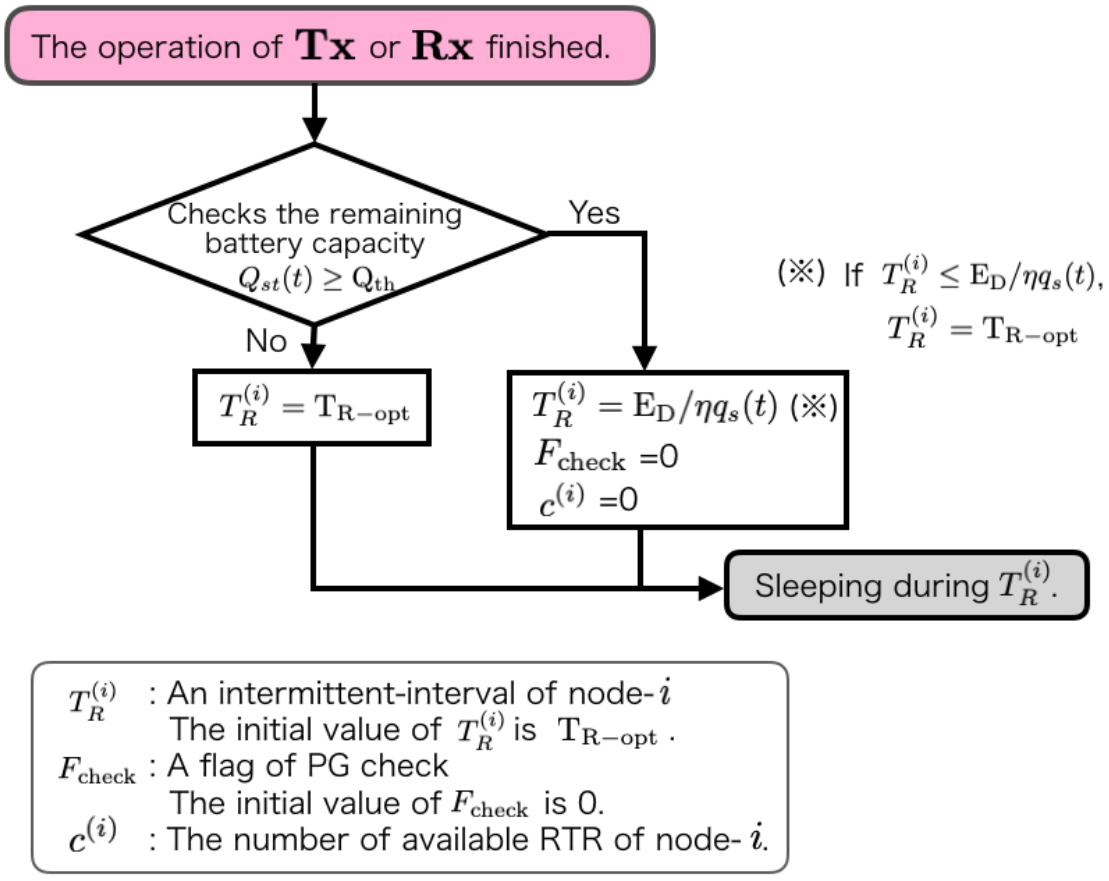

Figure 4.1: Operation of ENRI-MAC before going to sleep

4.2 Observation of peripheral condition

While the SN might have sufficient energy to forward more DATA packets, communication partners of that SN might not possess sufficient energy for transmission. Hence, when SN has gained more than the required energy for communication, it counts up the number of communicable nodes for a certain period of time to guarantee that it has a valid route to the GW. Figure 4.1 shows the operation at startup of ENRI-MAC.

When SNs whose storage capacity $Q_{st}(t)$ exceeds $\mathrm{Q_{ob}}$ wakes up from sleep, SNs listen surrounding signals for a certain period of $2\mathrm{T_{R-opt}}$. Let, $\mathrm{Q_{ob}}(t) = \mathrm{Q_{mid}} + 3\mathrm{E_D}$. $c^{(i)}$ represents the number of RTR which is transmitted from the lower cluster than own. If the SN cannot observe the number of RTR above $\mathrm{c_{th}}$, the SN is permitted to send DATA regardless of cluster. This load-unbalancing obviously prevents the outage of the network and thus results in the improvement of PLR. Next, we and the effect of load-unbalancing which could prevent the outage of network

Thus enables unbalance in the load, which is expected to be effective for preventing the outage of the network and improving PLR. show the evaluation of the performance of ENRI-MAC in a practical environment and the effect of load-unbalancing which could prevent the outage of network.

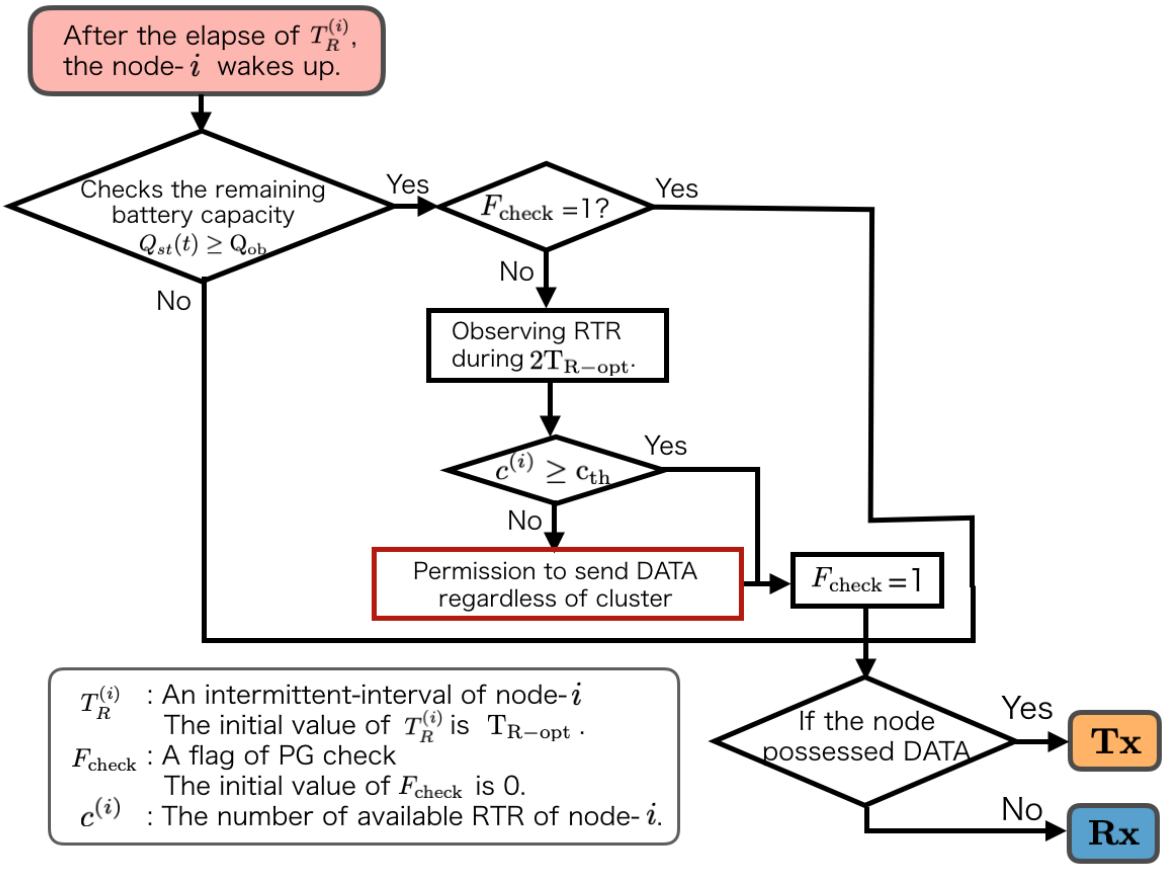

Figure 4.2: Operation at startup of ENRI-MAC

Chapter 5

Evaluation of Protocols with Empirical Model of Distributed Photovoltaics

In this chapter, we evaluate the performance of ENRI-MAC using the EH model based on actual measurement data. Since there are no stochastic power-supply model based on actual measurements for evaluation of our protocol, we focus on photovoltaics and attept to build an empirical model of EH. Concretely, we measured the illuminance during the day and made an empirical model of distributed photovoltaics. Next section describes the preparation of actual measurement model.

5.1 Experimental setup for evaluating

Based on the results of chapter 3.2., SNs were set up so where no isolated SNs would be generated. The number of SNs is 16. Figure 5.1 shows an actual network.

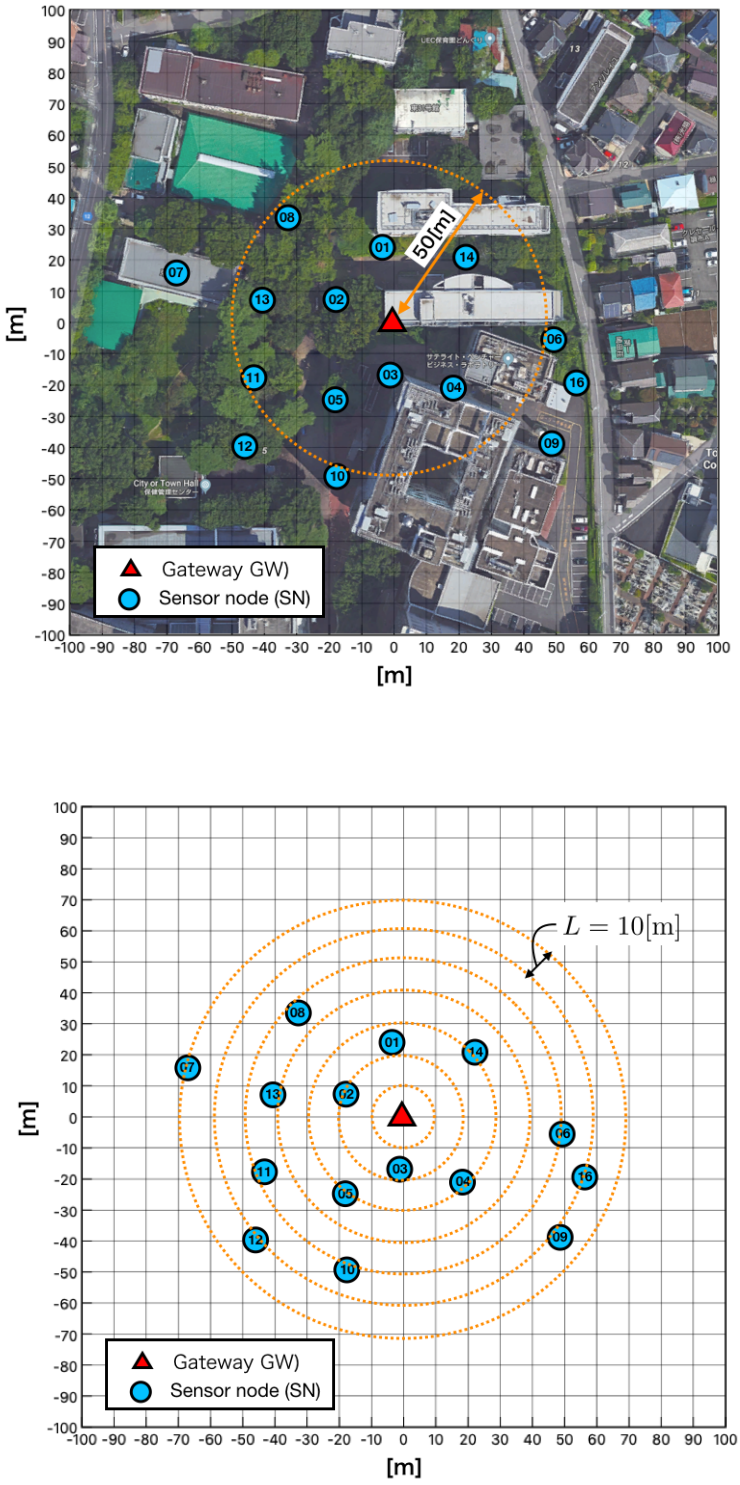

Figure 5.1: Network model of evaluation

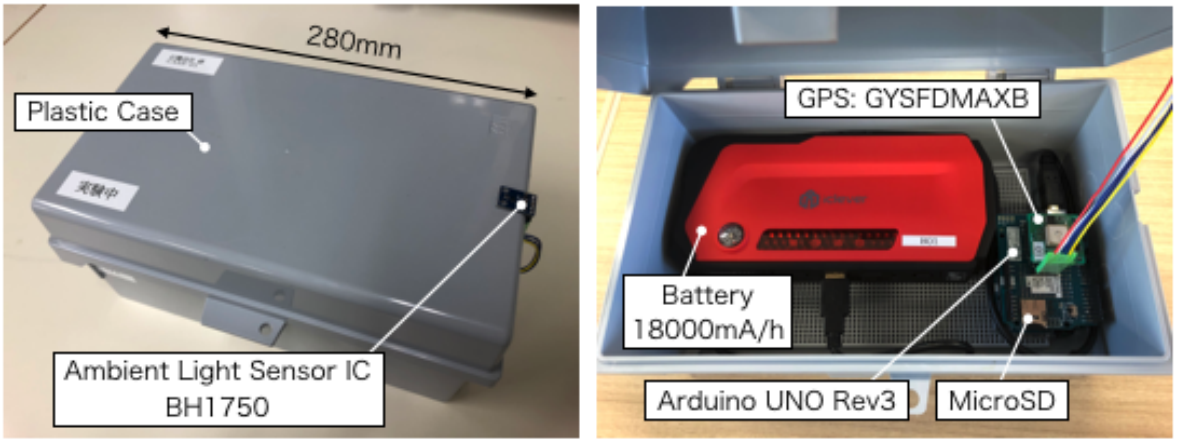

Figure 5.2: Experimental devices

Table 5.1: Experimental specification

Date	February 15, 2018
Central coordinates of the map in fig.5.1 (longitude, latitude)	(35.658499, 139.544233)
Weather	Cloudy
Temperature [°C]	$0 \sim 5.3$
Precipitation amount [mm]	0.0
Data Acquisition interval [sec]	1.0

5.2 Empirical Model of Energy Harvesting

In this section, we describe the empirical model of EH.

5.2.1 Experimental device

We measured illuminance during the day time using devices shown in 5.2. Sensors consists of with Arduino and I2C modules which can measure $0.01 \sim 54,612$[lx].

5.2.2 Photovoltaics output model

Actual Illuminance was measured with the arrangement in Figure 5.1. Experimental specification is show in table 5.1. Figure 5.3 shows illuminance during one day.

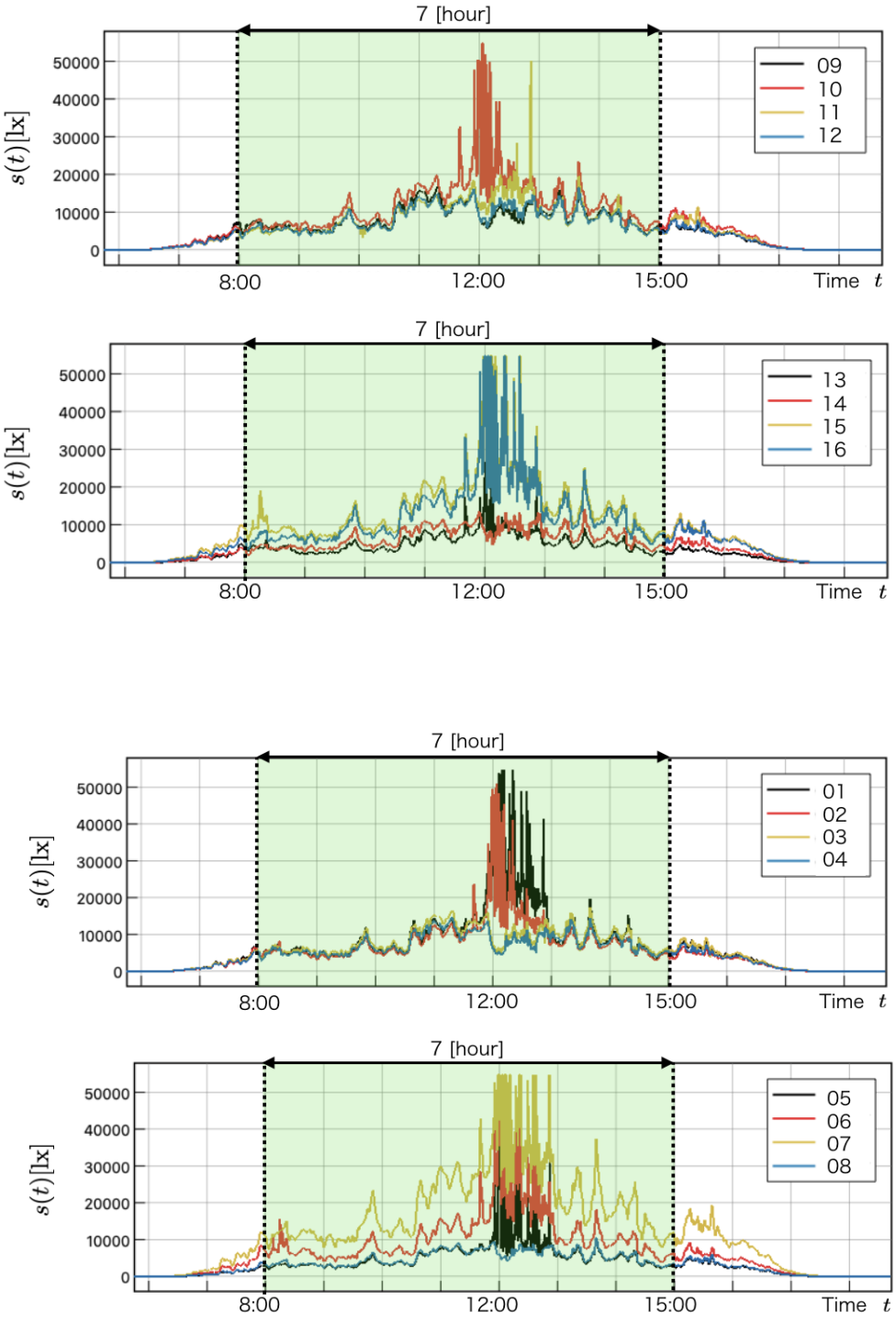

Figure 5.3: Actual illuminance

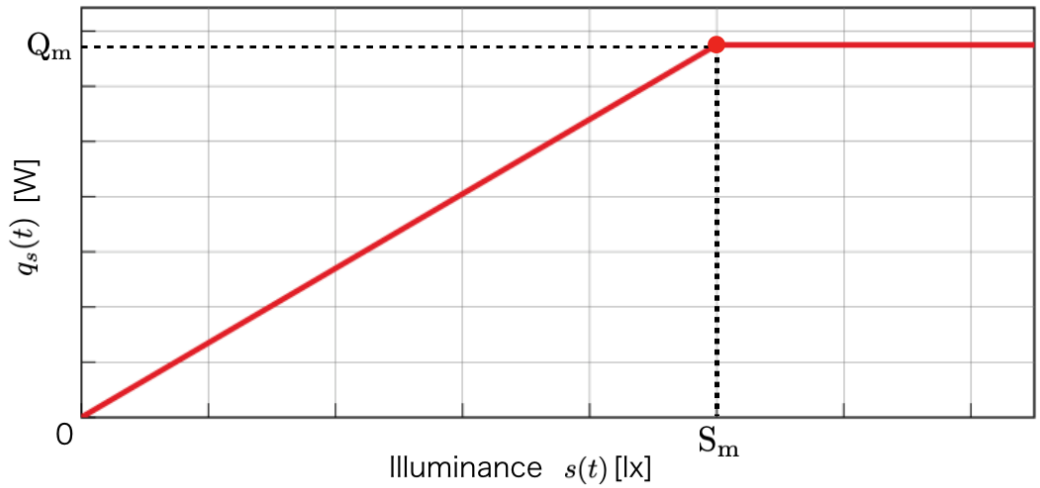

Figure 5.4: Photovoltaic output model

Based on the measured results, we calculate output power of photovoltaic using the following approximate equation,

$$q_s(t) \approx \begin{cases} \frac{s(t)}{\mathrm{S_m}} \mathrm{Q_m} & (s(t) \leq \mathrm{S_m}) \\ \mathrm{Q_m} & (\text{otherwise}). \end{cases} \tag{5.1}$$

It is considered that the output always achieves maximum efficiency using maximum power point tracking (MPPT) algorithm [12]. Figure 5.4 shows an assumed conversion model among illuminance and output power.

Table 5.2: Simulation parameter for evaluation with empirical model

The number of SNs	16
$T_R^{(i)}$ of IRDT [6] [msec]	500
Minimum $T_R^{(i)}$ of ENRI-MAC [7] T_S [msec]	500
Minimum $T_R^{(i)}$ of improved ENRI-MAC T_{R-opt} [msec]	500
Maximum $T_R^{(i)}$ of improved ENRI-MAC T_{R-MAX} [min]	10
Threshold of illuminance S_m [lx]	50,000
Maximum output Q_m [mW]	13.5
Average current during sleeping [nA]	20.0
Operating voltage [V]	$3.0 \sim 3.6$
The maximum capacity of super-capacitor [F]	1.0
Maximum charged amount of battery Q_{max} [mJ]	6,480
Initial charged amount of battery and Threshold Q_{mid} [mJ]	5,445
Outage charged amount of battery Q_{out} [mJ]	4,500

5.3 Numerical results

The simulation parameters are shown in Table 5.2 and the basic parameters are same as Table 3.1. In addition, we use an arbitrary value T_L. We evaluate the performance of PDR from 8 AM to 3 PM with aforementioned parameters. In this simulation, it is assumed that DATA packet loss occurs when packet collision occurs or the battery outage happens due to the amount of charge of the capacitor falls below Q_{out}.

Figure 5.5 shows PDR of IRDT, ENRI-MAC, and improved ENRI-MAC. As shown in Fig.5.5, PDR of ENRI-MAC and improved ENRI-MAC are higher than that of IRDT, especially, in the region, the regime where the harvested energy is low.

In terms of the parameter of long intermittent interval T_S of ENRI-MAC, if we fail to design the long intermittent interval properly, ENRI-MAC may cause a catastrophic situation that nodes in the coverage would run out of their batteries due to the chain reaction of energy scarcity through autonomous control of intermittent interval. While ENRI-MAC needs accurate design, improved ENRI-MAC achieves higher communication reliability without complex intermittent interval design.

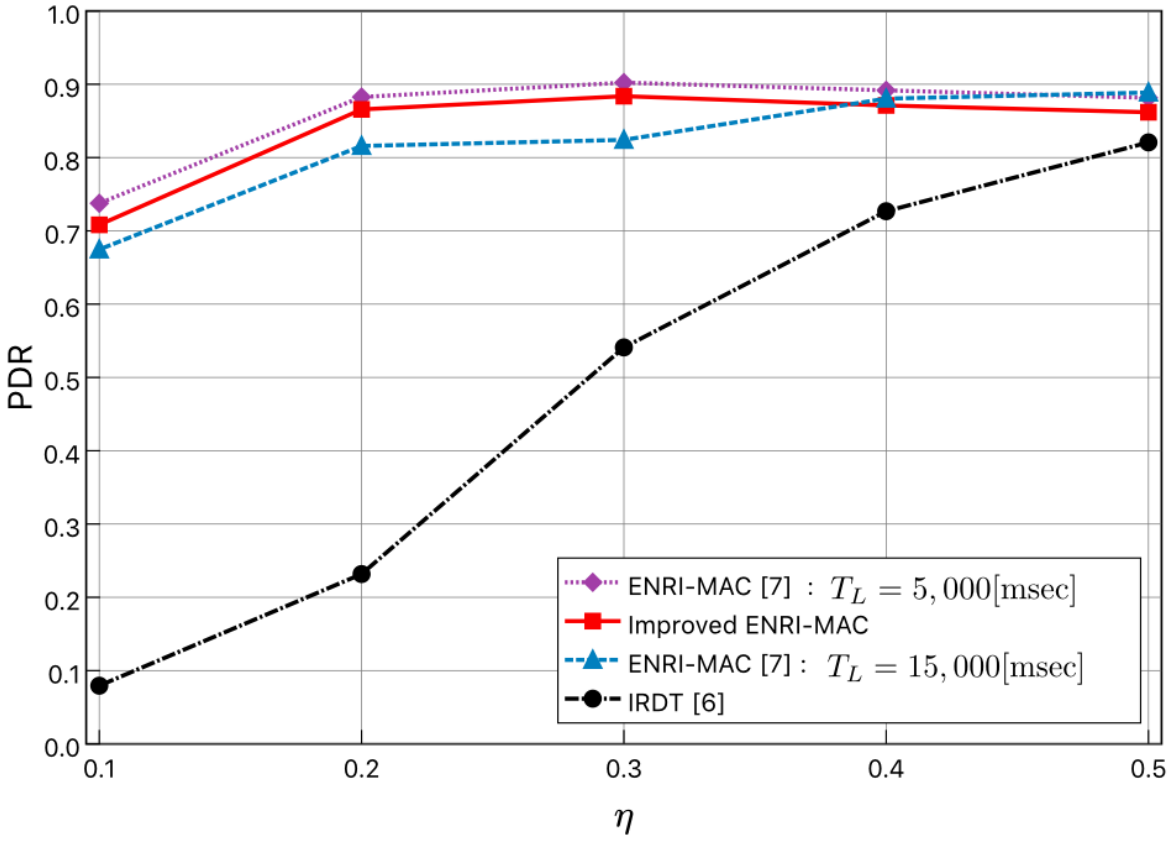

Figure 5.5: PDR of MAC protocols

Chapter 6

Conclusions

We evaluated the performance of improved ENRI-MAC using the energy-harvesting model based on actual measurement data. As a result, we show that improved ENRI-MAC protocol achieves high communication reliably in terms of PDR by the effectiveness of energy-neutral control system. On the other hand, it can be said that ENRI-MAC also achieves better performance if it can design the long intermittent interval properly. Note that, we assume that each SN can know the information on instantaneous harvested power and the remaining battery capacity in this paper. However, when we implement the system, it is difficult to know these information, so that we need the feasible method of deciding the long intermittent interval.

Appendix

This chapter describes experiments and implementations done in pursuing feasibility of EHWSNs.

A. Implementation of EHWSNs

We implement the ENRI-MAC [7] using Lazurite 920J manufactured by LAPIS Semiconductor Co., Ltd. Also, we propose and fabricate a power-good (PG) circuit, which outputs PG signal when the output voltage from the energy harvester exceeds the given threshold. Figure 6.1 shows the fabricated device. The detailed specification of the device is shown in Table 6.1. It is noteworthy that the system can be used with any kind of EH supplies such as radio-frequency signals and is remarkably low-cost since we only use general devices on the market while devices stably work only with EH power sources.

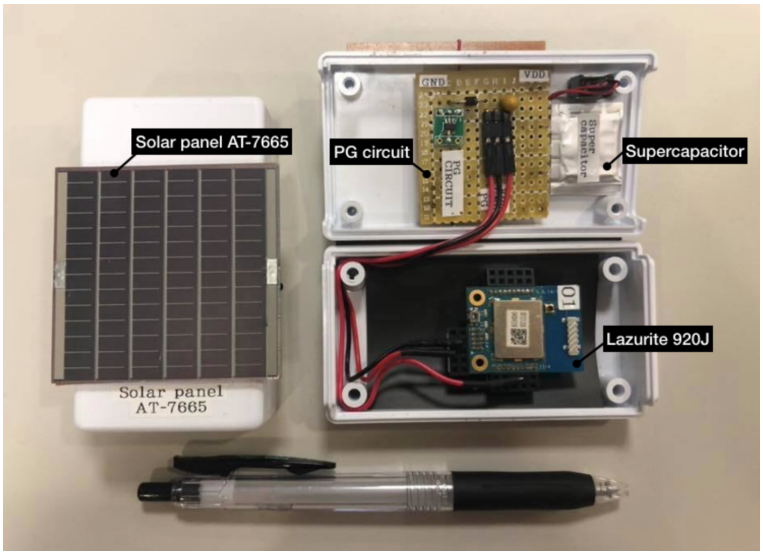

Figure 6.1: Lazurite 920J with solar panel AT-7665.

Table 6.1: Specification of Lazurite 920J

Transmitted power [mW]	1.0
Transmission rate [kbps]	100
Frequency band [MHz]	920
Frequency deviation [ppm]	±20 or less
Modulation	Binary GFSK
Antenna gain [dBm]	-1.8
Antenna receive sensitivity [dBm]	-100
Wireless standard	IEEE802.15.4g

We tried to show the demonstration at the conference venue of IEEE CCNC 2018. Note that, at the conference venue of IEEE CCNC 2018, we cannot use Lazurite 920J due to the radio regulations in the United States. Therefore, instead of demonstrating the prototype system, a recorded video of the demonstration described above was played together with prototype devices.

We explain a demonstration of the maintenance-free WSNs. Overall demonstration image is shown in Fig. 6.2. Also, table 6.2 shows demonstration parameters. The prototype devices are installed in practical environment as shown in Fig. 6.3. We use seven SNs to show the multi-hop capability of our system. Every node except Node-7 has EH power supply as shown in Fig. 6.1 and operates according to the proposed protocol. Only Node-7 generates DATA packets every one minute. Each DATA packet consists of 25 bytes whose payload is 18 bytes. Remaining part is used for a 5-byte header and 2-byte cyclic redundancy code (CRC). When Node-7 generates the packet, it writes its own unique ID (1 byte), a timestamp (7 bytes), an empty region as route-recording space (8 bytes), and a counter (2 bytes). When SN receives the DATA packet, it uses the empty sub-space of route-recording space; SN writes its own ID and its state of the PG signal in the sub-space (1 byte). By analyzing these data at the GW, we can know actual routes of every packets and nodes' states.
Figure 6.4 shows an example of actual output in a terminal after the transmission. As clear from the figure, the actual route of every transmission can be easily analyzed at the destination. In this case, the transmitted DATA packet from Node-7 was forwarded by Node-4 and Node-1. Also, nodes with PG signals more frequently contribute the transmission than ones without PG signals. From the figure, PG signal was active at Node-4. This observation confirms the conclusion obtained in chapter 6.

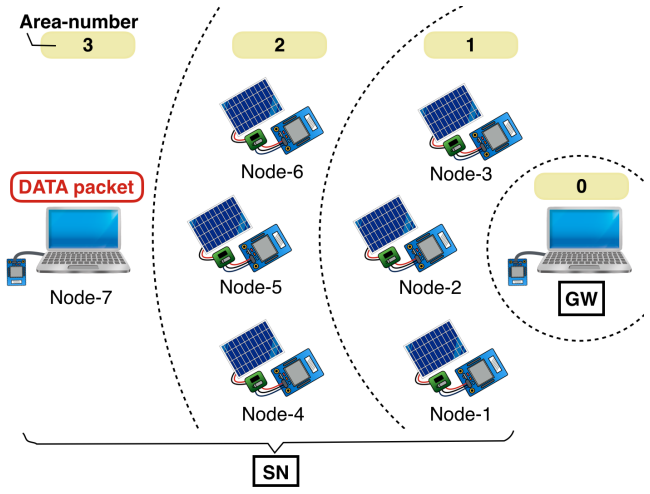

Figure 6.2: Demonstration image of our system.

Table 6.2: Demonstration Parameters

The number of sensor nodes	7
DATA packet generating interval T_g [min]	1.0
Size of DATA packet [byte]	25

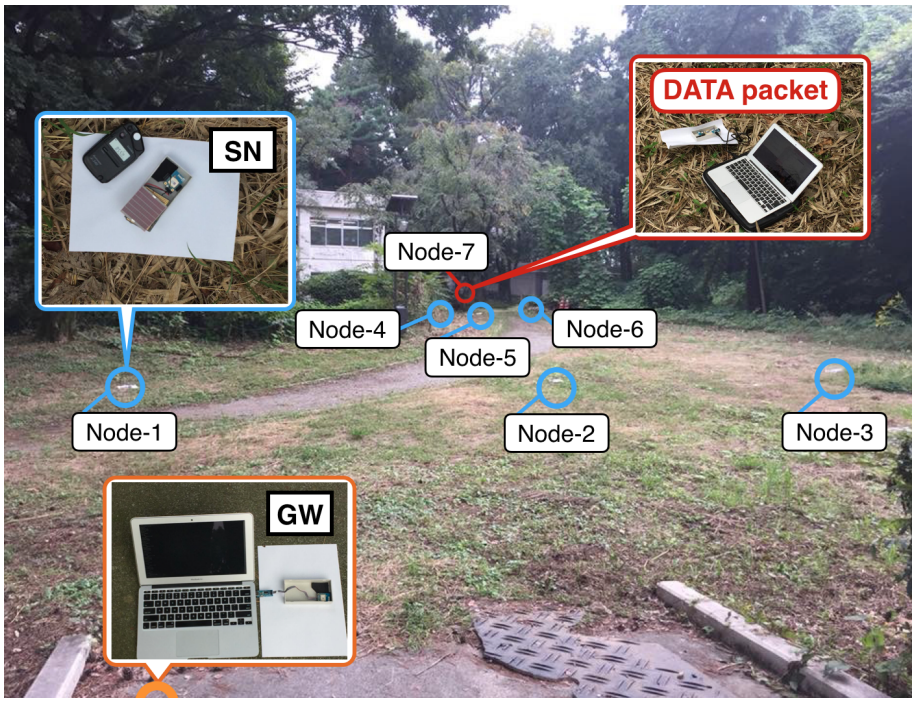

Figure 6.3: Demonstration system in practical environment.

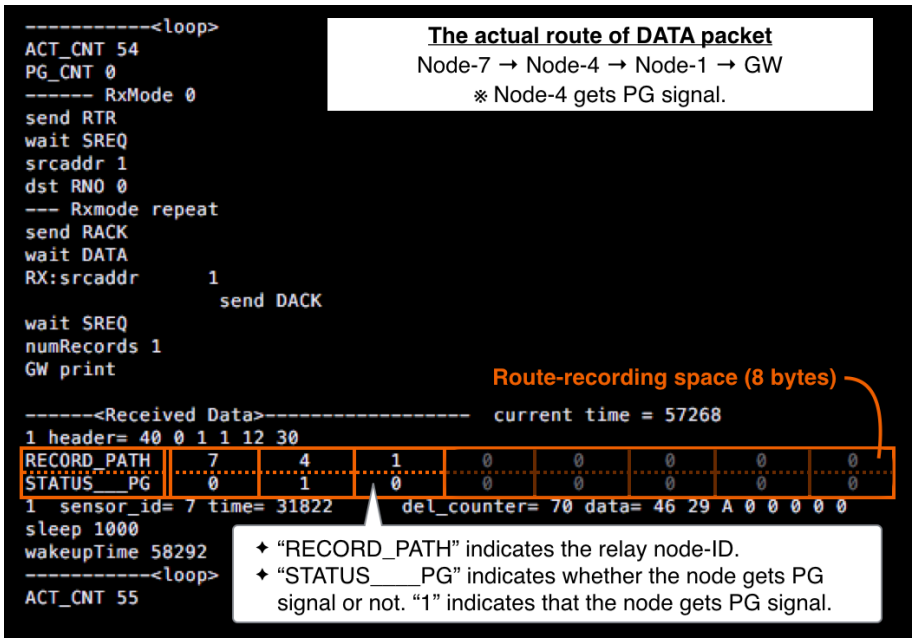

Figure 6.4: An example of terminal output in the demonstration system.

Bibliography

[1] I. F. Akyildiz, Weilian Su, Y. Sankarasubramaniam and E. Cayirci, "A survey on sensor networks,"*in IEEE Commun. Mag.*, vol. 40, no. 8, pp. 102–114, Aug. 2002.

[2] S. C. Ergen and P. Varaiya, "On Multi-Hop Routing for Energy Efficiency,"*IEEE Commun. Lett.*, vol.9, no.10, pp.880–881, May. 2005.

[3] V. Raghunathan, S. Ganeriwal, and M. Srivastava, "Emerging Techniques for Long Lived Wireless Sensor Networks,"*IEEE Commun. Mag.*, pp.108–114, Apr. 2006.

[4] W. Ye, J. Heidemann and D. Estrin, "Medium access control with coordinated adaptive sleeping for wireless sensor networks,"*in IEEE/ACM Trans. on Netw.*, vol. 12, no. 3, pp. 493–506, June 2004.

[5] Y. Sun, O. Gurewitz and D. B. Johnson, "RI-MAC: A receiver-initiated asynchronous duty cycle MAC protocol for dynamic traffic loads in wireless sensor networks," in Proc. *Int'l Conf. Embedded Netw. Sensor Syst.*, pp. 1–4, Nov. 2008.

[6] D. Kominami, M. Sugano, M. Murata, and T. Hatauchi, "Energy-efficient receiver-driven wireless mesh sensor networks," *Sensors 2011*, pp.111–137, Dec. 2010.

[7] R. Tanabe, T. Kawaguchi, R. Takitoge, K. Ishibashi, and K. Ishibashi, "Energy-Aware Receiver-Driven Medium Access Control Protocol for Wireless Energy-Harvesting Sensor Networks," in Proc.*IEEE Consum. Commun. & Netw. Conf.*, LasVegas, NV, pp. 1–6, Jan. 2018.

[8] ROHM, 920MHz 帯特定小電力無線モジュール BP3596A
https://www.rohm.co.jp/datasheet/BP3596A/bp3596a-j [2019.3.14 available]

[9] M. Haenggi, "Stochastic Geometry for Wireless Networks",*1st ed. Cambridge, U.K.: Cambridge Univ. Press*, 2012.

[10] T. Hatauchi, Y. Fukuyama, M. Ishii and T. Shikura, "A power efficient access method by polling for wireless mesh networks,"*IEEJ Trans. Electron. Inform. Syst.*, vol. 128, no. 12, pp. 1761–1766, Dec. 2008.

[11] 田邉稜，"エナジーハーベスティング電源のための適応的受信機駆動型 MAC プロトコルに関する研究"，電気通信大学 修士論文, Mar. 2018.

[12] M. G. Villalva, J. R. Gazoli and E. R. Filho, "Comprehensive Approach to Modeling and Simulation of Photovoltaic Arrays,"*in IEEE Trans. on Power Electronics*, vol. 24, no. 5, pp. 1198–1208, May 2009.

Acknowledgments

This thesis consists of my study in master degree at the University of Electro-Communications, Tokyo, Japan. I am grateful to a large number of people who have helped me to accomplish my work. First of all, I would like to express my deepest gratitude to my supervisor, Associate Professor Koji Ishibashi, for guiding throughout my work. His motivations and encouragements immensely helped me throughout my whole life in the University of Electro-Communications. I also would like to give my special thanks to Professor Yasushi Yamao, Professor Takeo Fujii, and Associate Professor Koichi Adachi for their valuable guidances, instruction and continuous supports.

This thesis contains the contributions of our collaborative research with the Communications & Networking (CNN) Laboratory @ Dankook University. During my stay at the university as a visiting scholar, I became indebted to Prof. Won-Yong Shin and students. Thanks to their warm and welcoming attitudes, I was able to focus on my research topic and explore a new research field.

In addition, I am grateful to the students and researchers who provided insightful comments at the international and domestic conferences.

I also grateful to all the members of advanced wireless communications and research center (AWCC), especially Mr. Manato Takai, Shun Ogata, Ryo Tanabe, Kazuya Ohira, and Hara Takanori for their discussions and kindness. Finally, I would like to thank my family for their words, attitudes, and every supports.

List of Publications

International Conference (peer-reviewed) (3)

1. T. Kawaguchi, R. Tanabe, R. Takitoge, K. Ishibashi, and K. Ishibashi, "Implementation of Condition-Aware Receiver-Initiated MAC Protocol to Realize Energy-Harvesting Wireless Sensor Networks," in Proc. *IEEE CCNC 2018*, Las Vegas, NV (2018. 1)

2. R. Tanabe, T. Kawaguchi, R. Takitoge, K. Ishibashi, and K. Ishibashi, "Energy-Aware Receiver-Driven Medium Access Control Protocol for Wireless Energy-Harvesting Sensor Networks," in Proc. *IEEE CCNC 2018*, Las Vegas, NV (2018. 1)

3. C. Tran, M. D. Nguyen, T. Kawaguchi, K. Ishibashi, and W.-Y. Shin, "Analysis of the received signal strength indicator in space and time," in Proc. *International Conference on Next Generation Computing (ICNGC)*, Vung Tau, Vietnam (2018. 12)

International Conference (4)

1. T. Kawaguchi and K.Ishibashi, "Empirical Model of Distributed Photovoltaics for Energy-Harvesting Wireless Communications", in Proc. *SmartCom 2018* (IEICE Tech. Rep.), vol. 118, no. 274, SR2018–84, pp. 61–62, Bangkok, Thailand (2018. 10)

2. T. Kawaguchi, R. Tanabe, and K. Ishibashi, "Experimental Evaluation of Condition-Aware Receiver-Initiated MAC Protocol for Energy-Harvesting Wireless Sensor Networks," in Proc. *SmartCom 2017* (IEICE Tech. Rep.), vol. 117, no. 257, SR2017–92, pp. 71-72, Rome, Italy (2017. 10)

3. C. Tran, M. D. Nguyen, T. Kawaguchi, K. Ishibashi, and W.-Y. Shin, "Statistical analysis of the received signal pattern in space and time," in Proc. *Korean Institute of Communications and Information Sciences (KICS) Winter Conference*, Pyeongchang, Korea, (2019. 1)

4. M. D. Nguyen, C. Tran, T. Kawaguchi, R. Tanabe, M. Oinaga, R. Takahashi, K. Ishibashi, and W.-Y. Shin, "Energy-aware receiver-driven medium access control protocol for wireless energy-harvesting sensor networks with multiple gateways," in Proc. *Korean Institute of Communications and Information Sciences (KICS) Winter Conference*, JeongSeon, Korea, (2018. 1)

Domestic Conference (4)

1. 川口達広, 田邉稜, 石橋功至, “太陽光発電の実計測データに基づく適応的受信機駆動型 MAC プロトコルの特性評価”, 情報理論とその応用シンポジウム 2018, pp263–pp268, いわき市, (2018.12)

2. 川口達広, 田邉 稜, 石橋功至, “[技術展示] Energy-Neutral Receiver-Initiated (ENRI) MAC プロトコルに基づくバッテリーレス無線センサネットワーク,”信学技報, vol. 118, no. 58, SR2018–20, pp. 115–119, (2018.5) [2018 年度 スマート無線研究会 技術特別賞]

3. 川口達広, 田邉稜, 石橋功至, “エナジーハーベスティングセンサーネットワークの実現に向けた受信機駆動型 MAC プロトコルの実装と実験的評価”, 信学技報, vol. 117, no. 132, RCS2017–109, pp. 97–102, (2017.7)

4. 田邉稜, 川口達広, 石橋功至, “エネルギーの流入出量に基づく分散間欠間隔制御付き受信機駆動型 MAC プロトコル”, 情報理論とその応用シンポジウム 2017, pp. 559–564, 新発田市, (2017.11–12)